Electronic Supplementary Material (ESI) for Journal of Materials Chemistry A.
This journal is © The Royal Society of Chemistry 2023

D-Calcium Pantothenate-derived Porous Carbon: Carbonization Mechanism and Application in aqueous Zn-ion Hybrid Capacitors

*Lanta Liu [a, b, c, 1], Ziyu Sun [a, 1], Yaping Lu [a], Jiapeng Zhang [a],Yiming Li [a] ,Gaixia Zhang [d, *], Xiaohong Chen [a, *], Sasha Omanovic [b], Shuhui Sun [c, *], and Huaihe Song [a, *]*

a State Key Laboratory of Chemical Resource Engineering, Beijing Key Laboratory of Electrochemical Process and Technology for Materials, Beijing University of Chemical Technology, Beijing, 100029, P. R. China.

b Department of Chemical Engineering, McGill University, 3610 Rue University, Quebec H3A 0C5, Canada.

c Institut National de la Recherche Scientifique (INRS), Énergie Matériaux Télécommunications Research Centre, Québec J3X 1P7, Canada.

d Department of Electrical Engineering, École de Technologie Supérieure (ÉTS), Montréal, Québec H3C 1K3, Canada.

E-mail: gaixia.zhang@etsmtl.ca, chenxh@mail.buct.edu.cn, shuhui.sun@inrs.ca, songhh@mail.buct.cn.

Equations for calculating specific capacitance, energy density, and power density

In a symmetric supercapacitors system, the specific capacitance (C_s, F g^{-1}), energy density (E, Wh kg^{-1}) and power density (P, W kg^{-1}) were calculated from the galvanostatic charging/discharging curves, employing the following equations, respectively:

$$C_s = \frac{2 \times I \times \Delta t}{m \times \Delta V}$$

$$E = \frac{C_s \times \Delta V^2}{2 \times 4 \times 3.6}$$

$$P = \frac{3600E}{\Delta t}$$

where I (A) represents the discharge current, Δt (s) refers to the discharge time, m (g) indicates the mass of the active material, and ΔV is the voltage window including the voltage drop.

In a Zn-ion capacitor system, the specific capacitance (C_s, F g^{-1}), energy density (E, Wh kg^{-1}) and power density (P, W kg^{-1}) were calculated employing the following equations:

$$C_s = \frac{I \times \Delta t}{m \times \Delta V}$$

$$E = \frac{C_s \times \Delta V^2}{2 \times 3.6}$$

$$P = \frac{3600E}{\Delta t}$$

where I (A) represents the discharge current, Δt (s) refers to the discharge time, m (g) indicates the mass of the active material, and ΔV is the voltage window including the voltage drop.

Calculation details

All the DFT calculations were carried out by DMol3 of Materials Studio 2017 software. All calculations are performed using the exchange correlation term of the GGA (general gradient approximation) in spin-unrestricted and the PBE (Perdew-Burke-Ernzerhof) exchange related functionals, and the method proposed by Grimme (DFT-D2) takes into account the effect of dispersion. The basis set adopts the DNP (Double Numerical plus polarization) with polarization function and combines the effective potential DSPP approximation processing method, replacing the core electrons with a single effective potential and introduces a relativistic correction.

All-electron calculations were carried out with double numerical plus polarization (DNP). k-points were set as 2*2*1 for structural configuration optimizations. The convergence in energy, maximum force, and self-consistent field convergence threshold were set as 10^{-5} Ha, 10^{-3} Ha/Å, and 10^{-6} Ha, respectively. The global orbital cutoff was 6 Å. In order to avoid periodic mirroring, a 20 Å vacuum layer is used.

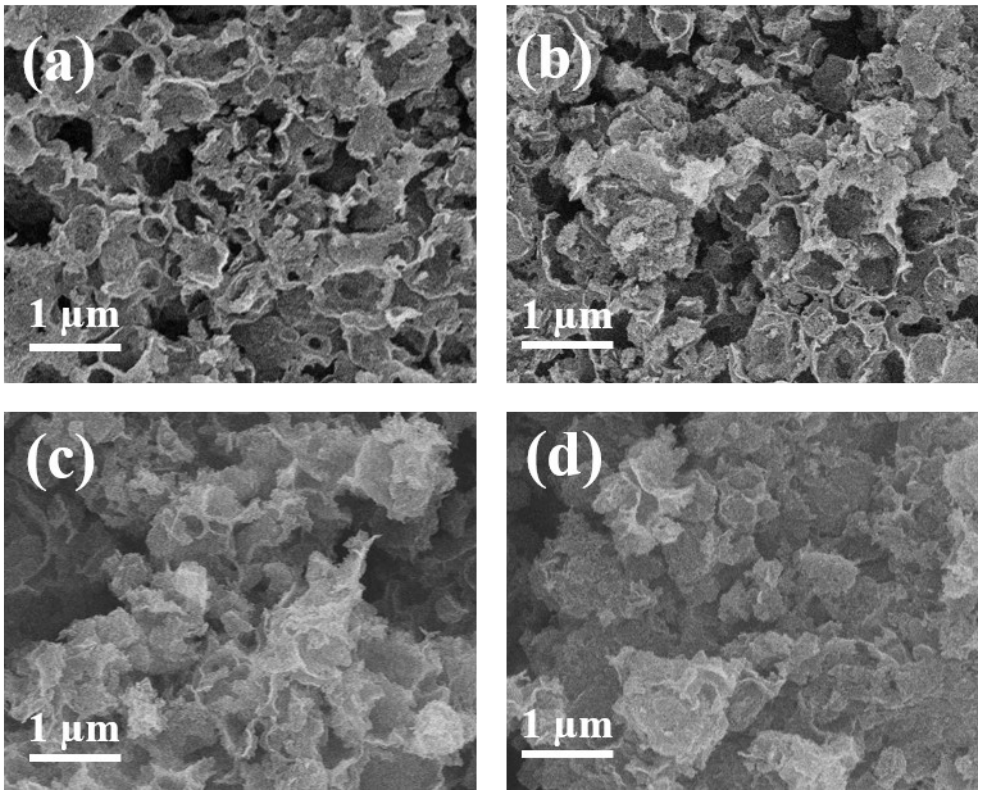

Figure S1. Micromorphology of DPC-X samples after HCl washing: (a) 700 ℃, (b) 800 ℃, (c) 900 ℃, (d) 1000 ℃.

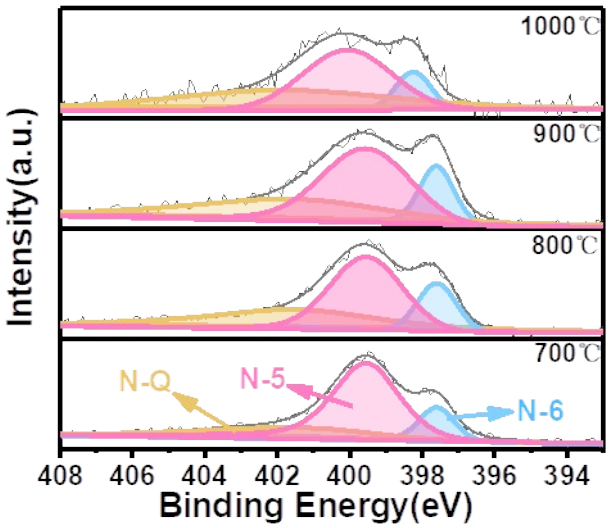

Figure S2. Deconvolution N 1s XPS spectra.

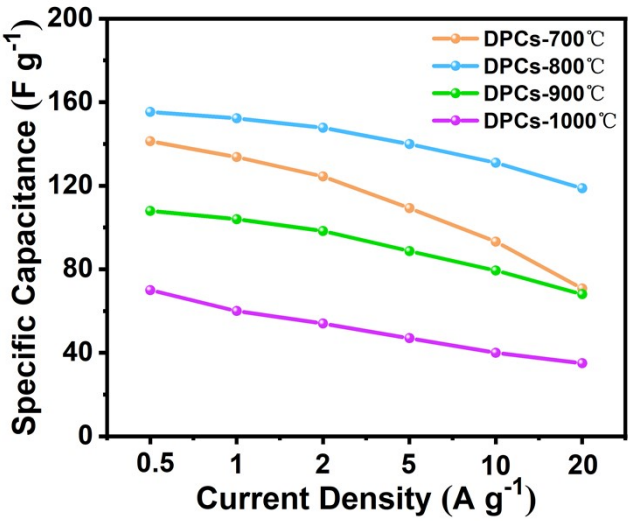

Figure S3. Rate performance of DPCs-X in symmetric supercapacitors.

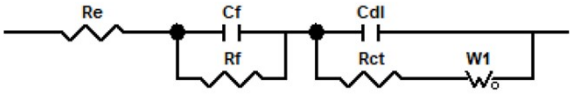

Sample	Re / Ω	Rf / Ω	Rct / Ω
DPCs-700℃	0.6402	0.7905	1.094×10^{-9}
DPCs-800℃	0.5909	0.3952	1.473×10^{-7}
DPCs-900℃	1.263	0.1820	1.661×10^{-6}
DPCs-1000℃	1.481	0.3706	2.486×10^{-9}

Figure S4. Fitting results of EIS of DPCs-X in symmetric supercapacitors.

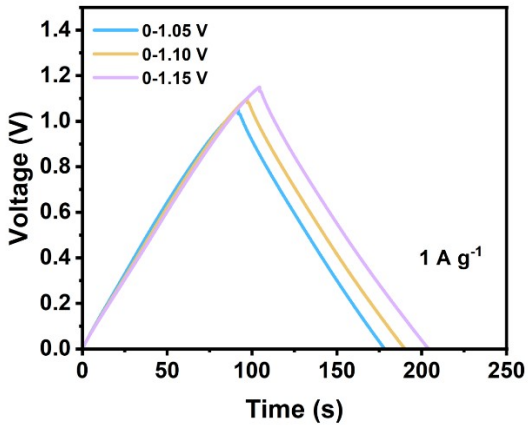

Figure S5. GCD curves of different voltage windows at 1 A g^{-1}.

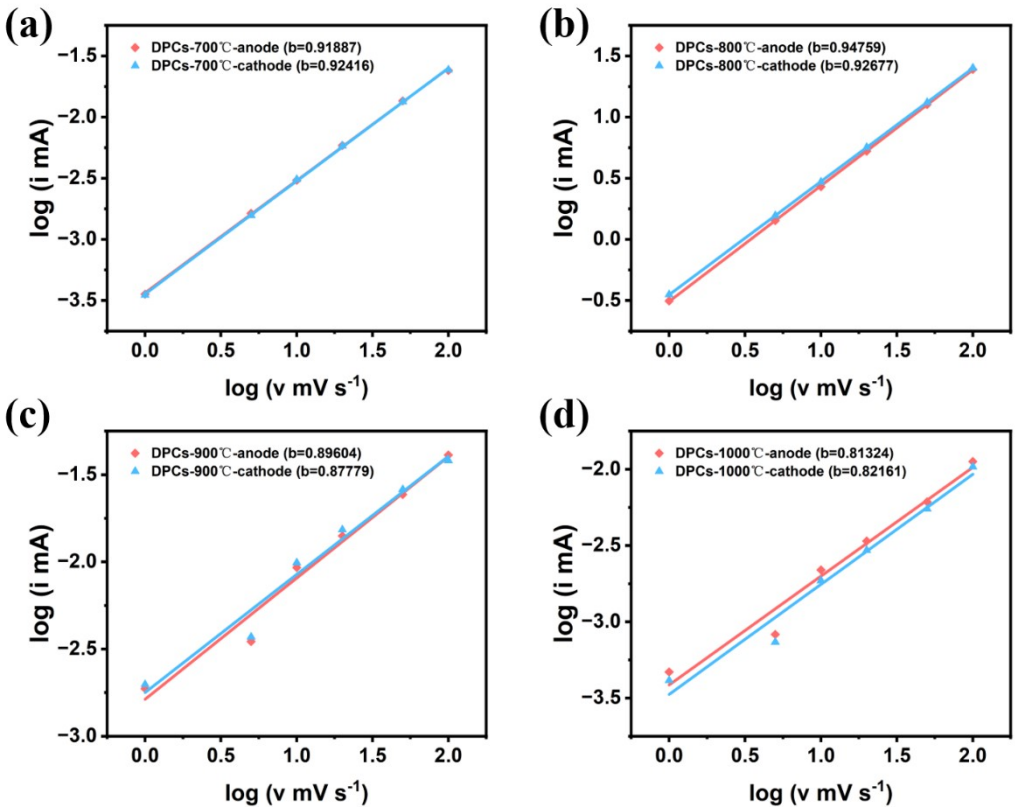

Figure S6. b-values of DPCs-X in ZIHCs.

The relationship between peak current (i) and scan rate (v) can be expressed in the following formula:

$$i = av^b$$

$$\log(i) = b\log(v) + log(a)$$

where a and b are the adjustable parameters. Generally, a b value of 0.5 represents a diffusion-controlled intercalation energy storage process, and a b value of 1 indicates a capacitive-dominated adsorption process.

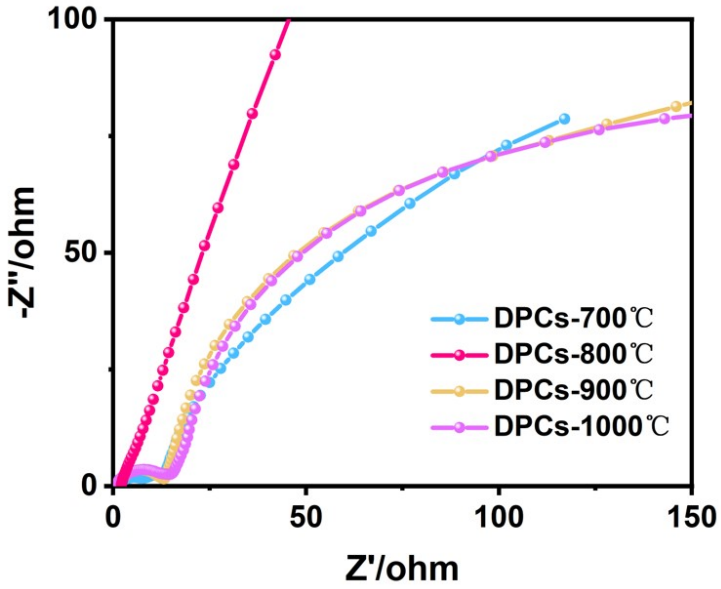

Figure S7. Nyquist plots of DPCs-X in ZIHCs

Table S1. Specific surface area and pore structure parameters of different DPC-X samples.

Sample	S_{BET}[a] ($m^2 g^{-1}$)	S_{micro}[b] ($m^2 g^{-1}$)	S_{EXT}[c] ($m^2 g^{-1}$)	Pore[d] Size(nm)	V_{pore}[e] ($cm^3 g^{-1}$)	V_{micro}[f] ($cm^3 g^{-1}$)
700	458.3	202.5	245.6	8.5	0.9	0.10
800	1422.9	426.8	1688.1	6.6	2.4	0.39
900	401.9	68.9	337.0	12.6	1.3	0.03
1000	465.1	35.0	428.7	16.5	1.9	0.01

Table S2. Elemental composition of DPC-X samples obtained from XPS spectra.

Sample	C(at.%)	N(at.%)	O(at.%)	N components at % of total N1s		
				N-6	N-5	N-Q
700	82.5	8	9.5	2.1	4.2	1.7
800	85.3	6.7	8	2.0	3.0	1.7
900	88.0	5.9	6.1	1.6	2.6	1.7
1000	90.9	3.9	5.2	1.1	1.9	0.9

Table S3. Comparison of rate performance of ZIHCs.

Materials	Rate performance
This work	**140.0 mAh g^{-1} at 0.2 A g^{-1}** **121.2 mAh g^{-1} at 0.4 A g^{-1}** **103.5 mAh g^{-1} at 0.8 A g^{-1}** **98.9 mAh g^{-1} at 1.6 A g^{-1}** **90.1 mAh g^{-1} at 3.2 A g^{-1}** **86.2 mAh g^{-1} at 6.4 A g^{-1}**
Activated Carbon[1]	70.8 mAh g^{-1} at 0.1 A g^{-1} 66.7 mAh g^{-1} at 0.5 A g^{-1} 64.3 mAh g^{-1} at 1 A g^{-1} 60.7 mAh g^{-1} at 2 A g^{-1} 57.7 mAh g^{-1} at 5 A g^{-1}
Inconnected Porous Carbon[2]	86.7 mAh g^{-1} at 0.2 A g^{-1} 71.2 mAh g^{-1} at 0.4 A g^{-1} 60 mAh g^{-1} at 0.8 A g^{-1} 48.5 mAh g^{-1} at 1.6 A g^{-1} 44.8 mAh g^{-1} at 6.4 A g^{-1}
Polymer Carbon Spheres[3]	172 F g^{-1} at 0.13 A g^{-1} 129 F g^{-1} at 0.6 A g^{-1} 107 F g^{-1} at 1.13 A g^{-1} 97 F g^{-1} at 1.5 A g^{-1}
S,N-rich Porous Carbon Nanotubes[4]	120.3 mAh g^{-1} at 0.2 A g^{-1} 106.7 mAh g^{-1} at 0.5 A g^{-1} 69.5 mAh g^{-1} at 5 A g^{-1}
Ultrathin Carbon Nanosheets[5]	103 mAh g^{-1} at 0.1 A g^{-1} 81 mAh g^{-1} at 0.2 A g^{-1} 65 mAh g^{-1} at 0.5A g^{-1} 52 mAh g^{-1} at 1 A g^{-1} 49 mAh g^{-1} at 2 A g^{-1}
B, N-codoped MOF-based Carbon[6]	92.7 mAh g^{-1} at 1 A g^{-1} 81.6 mAh g^{-1} at 2 A g^{-1} 68.6 mAh g^{-1} at 4 A g^{-1} 59.4 mAh g^{-1} at 6 A g^{-1}
N-doped Porous Carbon[7]	120 mAh g^{-1} at 0.2 A g^{-1} 103 mAh g^{-1} at 0.5 A g^{-1} 79 mAh g^{-1} at 2 A g^{-1} 60 mAh g^{-1} at 5 A g^{-1}

1 C. Li, Z. Sun, T. Yang, L. Yu, N. Wei, Z. Tian, J. Cai, J. Lv, Y. Shao, M. H. Rummeli, J. Sun and Z. Liu, *Advanced Materials*, 2020, **32**, 2003425.

2 L. Liu, Y. Lu, D. Qiu, D. Wang, Y. Ding, G. Wang, Z. Liang, Z. Shen, A. Li, X. Chen and H. Song, *Journal of Colloid and Interface Science*, 2022, **620**, 284-292.

3 F.-Z. Cui, Z. Liu, D.-L. Ma, L. Liu, T. Huang, P. Zhang, D. Tan, F. Wang, G.-F. Jiang and Y. Wu, *Chemical Engineering Journal*, 2021, **405**, 127038.

4 J. Li, L. Yu, W. Wang, X. He, G. Wang, R. Liu, X. Ma and G. Zhang, *Journal of Materials Chemistry A*, 2022, **10**, 9355-9362.

5 Y. Zhang, Z. Wang, D. Li, Q. Sun, K. Lai, K. Li, Q. Yuan, X. Liu and L. Ci, *Journal of Materials Chemistry A*, 2020, **8**, 22874-22885.

6 L. Han, X. Zhang, J. Li, H. Huang, X. Xu, X. Liu, Z. Yang, M. Xu and L. Pan, *Journal of Colloid and Interface Science*, 2021, **599**, 556-565.

7 J. Li, J. Zhang, L. Yu, J. Gao, X. He, H. Liu, Y. Guo and G. Zhang, *Energy Storage Materials*, 2021, **42**, 705-714.